ISSN 1063-7834, Physics of the Solid State, 2010, Vol. 52, No. 2, pp. 357–363. © Pleiades Publishing, Ltd., 2010.
Original Russian Text © V.S. Zhandun, N.G. Zamkova, V.I. Zinenko, 2010, published in Fizika Tverdogo Tela, 2010, Vol. 52, No. 2, pp. 333–338.

LATTICE DYNAMICS AND PHASE TRANSITIONS

Lattice Dynamics and the Ferroelectric Phase Transition in Ordered $Pb_2B'B''O_6$ (B' = Ga, In, Lu; B'' = Nb, Ta) Solid Solutions

V. S. Zhandun, N. G. Zamkova, and V. I. Zinenko

Kirensky Institute of Physics, Siberian Branch, Russian Academy of Sciences, Akademgorodok 50, Krasnoyarsk, 660036 Russia

e-mail: jvc@iph.krasn.ru

Received May 12, 2009

Abstract—The lattice vibration spectrum, rf permittivity, and dynamic Born charges have been calculated for ordered $Pb_2B'B''O_3$ (B' = Ga, In, Lu; B'' = Nb, Ta) solid solutions in terms of the generalized Gordon–Kim model. It has been shown that all compounds exhibit a ferroelectric instability and that the frequencies of "soft" ferroelectric modes are close in magnitude. The ferroelectric phase-transition temperatures and the spontaneous polarization in the ferroelectric phase of the solid solutions under consideration have been calculated by the Monte Carlo method using the model Hamiltonian in the local mode approximation. The transition temperature is found to increase with increasing atomic number of the B' ion.

DOI: 10.1134/S1063783410020228

Solid solutions of oxides with the general formula ABO_3 have been extensively studied for several decades. Recently, the interest in these compounds has increased due to the new possibilities of their practical applications owing to their unusual phase diagrams and properties [1]. The lead-containing $PbB'_{1/2}B''_{1/2}O_3$ (B' = Sc, Ga, In, Lu; B'' = Nb, Ta) solid solutions exhibit interesting properties. The high-temperature phase of $PbB'_{1/2}B''_{1/2}O_3$ compounds disordered in cations B has a perovskite structure, whereas the high-temperature phase of the ordered solid solutions has an elpasolite structure ($Fm3m$). As the temperature decreases, the compounds, depending on the chemical composition and the degree of ordering of cations B' and B'', undergo either ferroelectric or antiferroelectric phase transitions. The solid solutions in which B' = Sc, such as $PbSc_{1/2}Nb_{1/2}O_3$ (PSN) and $PbSc_{1/2}Ta_{1/2}O_3$ (PST), have been studied most extensively. Both solid solutions undergo a ferroelectric phase transition to the rhombohedral phase with symmetry $R3$. In completely ordered Pb_2ScNbO_6 and Pb_2ScTaO_6, this transition is a sharp ferroelectric transition; as Sc and Nb(Ta) are disordered, the transition becomes diffuse and the compounds begin to manifest relaxor properties. The data on other compounds are much less available in the literature; for the most part, these are studies of $PbIn_{1/2}B''_{1/2}O_3$ (PIN and PIT) and $PbLu_{1/2}In_{1/2}O_3$ (PLN) [2–8]. There are experimental data which show that these compounds, unlike ferroelectrics PSN and PST, undergo an antiferroelectric transition and that transitions between the antiferroelectric and ferroelectric phases are possible [2, 9]. The mechanism of these transitions is not completely understood from both the experimental and theoretical standpoints.

The aim of this work is to calculate the lattice vibration spectrum, the ferroelectric phase transition temperature, and the spontaneous polarization for a number of ordered $Pb_2B'B''O_6$ (B' = Sc, Ga, In, Lu; B'' = Nb, Ta) solid solutions. The lattice dynamics and the ferroelectric phase transition for ordered scandium solid solutions were calculated in [10, 11]. Here, some results of the calculations are presented for completeness of the pattern of the properties of the compound series under study. For all disordered solid solutions, the lattice dynamics and the ferroelectric phase transition were calculated in [12].

In the framework of the generalized Gordon–Kim model with inclusion of the dipole and quadrupole polarizabilities of ions [13], the lattice dynamics was calculated for the ordered solid solutions with the elpasolite structure. In the elpasolite structure, the O^{-2} ions have a free coordinate related to displacements of the oxygen ions along the Ta(Nb)–O bond. The positions of the oxygen ions in the cubic phase were found from the minimum of the total energy. In all the compounds under consideration, the oxygen octahedron is displaced to the Ta(Nb) ion by approximately 0.08 Å. The unit cell parameters were also found by minimization of the total energy of the crystals; they are listed in Table 1 along with the known experimental values. The calculated unit cell parameters are less than experimental values by 1–3%. The calculations of the

Table 1. Experimental a_{exp} and calculated a_{min} equilibrium unit cell parameters (Å)

Compound	a_{min}	a_{exp}	Compound	a_{min}	a_{exp}
PSN	7.84	8.14 [14]	PST	7.98	8.14 [15]
PGN	7.96	8.18	PGT	8.08	8.18
PIN	8.08	8.22 [16]	PIT	8.14	8.16 [16]
PLN	8.18	8.3 [1]	PLT	8.24	8.26

lattice dynamics and energies of low-symmetric phases were performed based on the experimental values of the lattice parameters, because it is known that the ferroelectric instability is very sensitive to the unit cell volume. For the crystals with B' = Ga and $PbLu_{1/2}Ta_{1/2}O_3$, for which we did not find the experimental values of the unit cell parameter, the calculation was performed using the parameters equal to 8.14 and 8.26 Å, respectively.

In terms of this model, the rf permittivity, dynamic Born charges, and frequency spectra of the crystal lattice vibrations were calculated for the ordered solid solutions such as $PbGa_{1/2}Nb_{1/2}O_3$ (PGN), $PbGa_{1/2}Ta_{1/2}O_3$ (PGT), PIN, PIT, PLN, and PLT. It is seen from Table 2 that the dynamic charges of $\langle B\rangle$ and $O_{\parallel}$ ions decrease as the atomic number of the $\langle B\rangle$ ion increases, as was also noted in [10, 12] for the disordered solid solutions. Figure 1 depicts the

Table 2. Calculated values of the rf permittivity ε_∞, dynamic Born charges Z^{dyn} (in units of e), and frequencies of the soft ferroelectric mode ω_s (cm^{-1})

Compound	ε_∞	Z^{dyn}_{Pb}	$Z^{dyn}_{B'}$	$Z^{dyn}_{B''}$	$Z^{dyn}_{O_\parallel}$	$Z^{dyn}_{O_\perp}$	ω_s
PSN	3.5	2.70	4.2	5.96	–4.15	–1.82	–95
PGN	3.31	2.67	3.48	5.73	–3.3	–1.90	–62
PIN	3.1	2.70	3.25	6.1	–3.6	–1.95	–57
PLN	2.84	2.65	2.8	5.91	–2.8	–2.16	–61
PST	3.34	2.67	3.94	4.21	–2.68	–2.04	–62
PGT	3.2	2.65	3.3	4.2	–2.25	–2.08	–61
PIT	2.93	2.66	3.2	4.6	–2.22	–2.17	–65
PLT	3.09	2.63	2.55	4.32	–2.22	–1.62	–67

Table 3. Vibration frequencies (cm^{-1}) at $q = 0$ for the ordered $PbB'_{1/2}B''_{1/2}O_3$ solid solutions (the mode degeneration is indicated in parentheses, and the soft modes are represented by the negative values)

PSN	PGN	PIN	PLN	PST	PGT	PIT	PLT
–95.8(2)	–61.7(2)	–57.3(2)	–60.3(2)	–89.5(3)	–92.2(3)	–125.4(3)	–137.6(3)
–51.4(3)	–50.6(3)	–48.1(3)	–49.8(3)	–62.1(2)	–61.4(2)	–65.5(2)	–67.1(2)
69.0(3)	77.0(3)	43.5(3)	58.0(3)	–57.4(3)	–57.7(3)	–58.4(3)	–58.9(3)
78.5	90.3	96.6	90.4	106.6	106.6	103.5	99.6
120.0(2)	178.1(2)	185.8(2)	157.2(2)	183.7(3)	185.2(3)	176.2(3)	171.5(2)
202.8(3)	208.0(3)	207.7(3)	182.8	234.8(2)	222.1(2)	197.1(2)	173.8(3)
256.3(3)	242.0	215.2	213.6(3)	240.6	230.7	214.3	189.9
268.7	263.0(3)	269.3(3)	279.5(3)	246.2(2)	250.0(2)	254.7(2)	256.9(2)
296.0(2)	309.0(2)	315.8(2)	321.0(2)	251.6(3)	256.1(3)	259.5(3)	264.0(3)
309.2(2)	335.6(2)	358.5	368.8	361.4	352.0	348.2	358.8
339.3	345.2	427.5(2)	421.1(2)	475.1(2)	489.7(2)	533.6(2)	541.6(2)
375.3(2)	390.7(2)	432.2(2)	439.0(2)	529.6(2)	540.3(2)	567.0(2)	574.0(2)
510.3	515.3	550.9	534.2	578.0	577.0	597.5	593.3

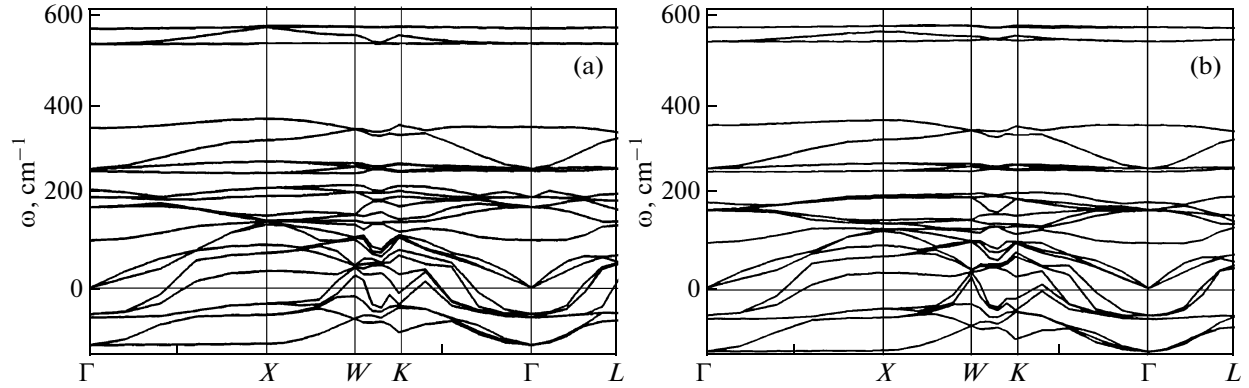

Fig. 1. Calculated phonon spectra of the ordered (a) PIT and (b) PLT solid solutions. The imaginary frequencies are represented by negative values.

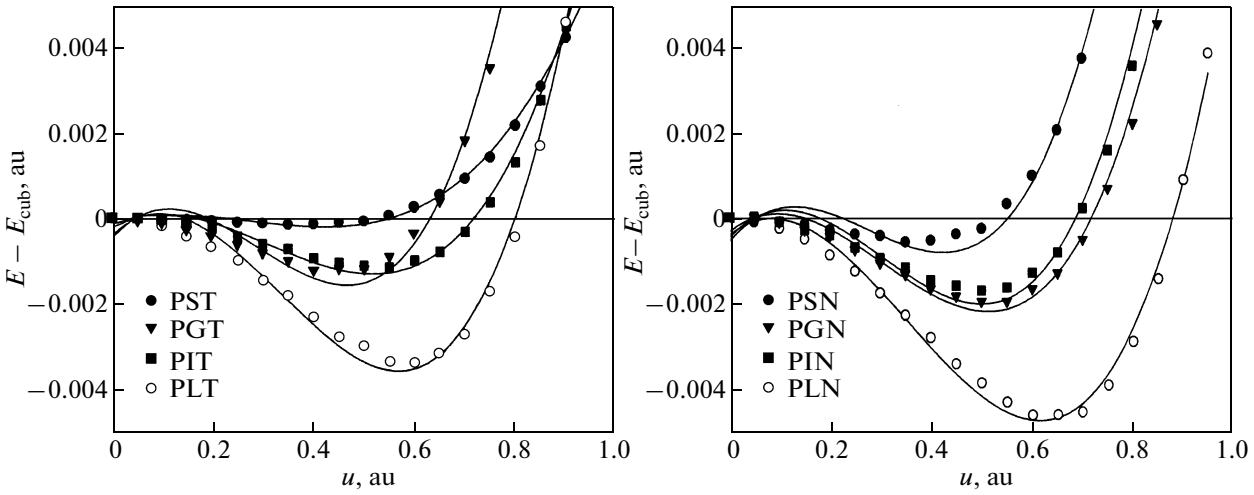

Fig. 2. Dependences of the difference between the total energies of the distorted and undistorted $Pb_2B'B''O_6$ solid solutions on the amplitude of ionic displacements along the eigenvector of the ferroelectric mode in the [111] direction.

total phonon spectra calculated for the PIT and PLT compounds; the calculations show that the spectra are qualitatively similar for all the compounds (the spectra for PSN and PST are presented in [10]); because of this we do not show the spectra for all the compounds to save room. It is seen from Table 3, in which the vibration frequencies in the Brillouin zone center are given, that all the $Pb_2B'B''O_6$ compounds have a soft vibrational mode with symmetry Γ_{15} corresponding to the ferroelectric instability of the lattice. The calculated eigenvectors of these unstable ferroelectric modes of the compounds under consideration are listed in Table 4. As seen, the Pb and $O_\perp$ ions have the largest displacements which are assumed to be related to the ferroelectric instability in the lead-containing crystals. These displacements are practically the same for all the compounds. It was detected as well that the frequencies of the ferroelectric modes for whole series of the ordered solid solutions are very close to each other. The vibration spectra of the crystal lattice obtained are little different in the cases of the ordered and disordered solid solutions [10].

As the crystal is distorted by the obtained eigenvector of the soft ferroelectric mode, the ion displacements along the space diagonals of the cubic unit cell (the [111] direction) are more energetically preferable, which corresponds to the rhombohedral phase symmetry. Figure 2 shows the dependences of the crystal energy counted from the energy of the undistorted cubic crystal ($E - E_{cub}$) on the amplitude of the ionic displacements along the eigenvector of the soft ferroelectric mode in the [111] direction. As seen from Fig. 2, the depth of the energetic minimum increases with increasing atomic number of the B' ion and is

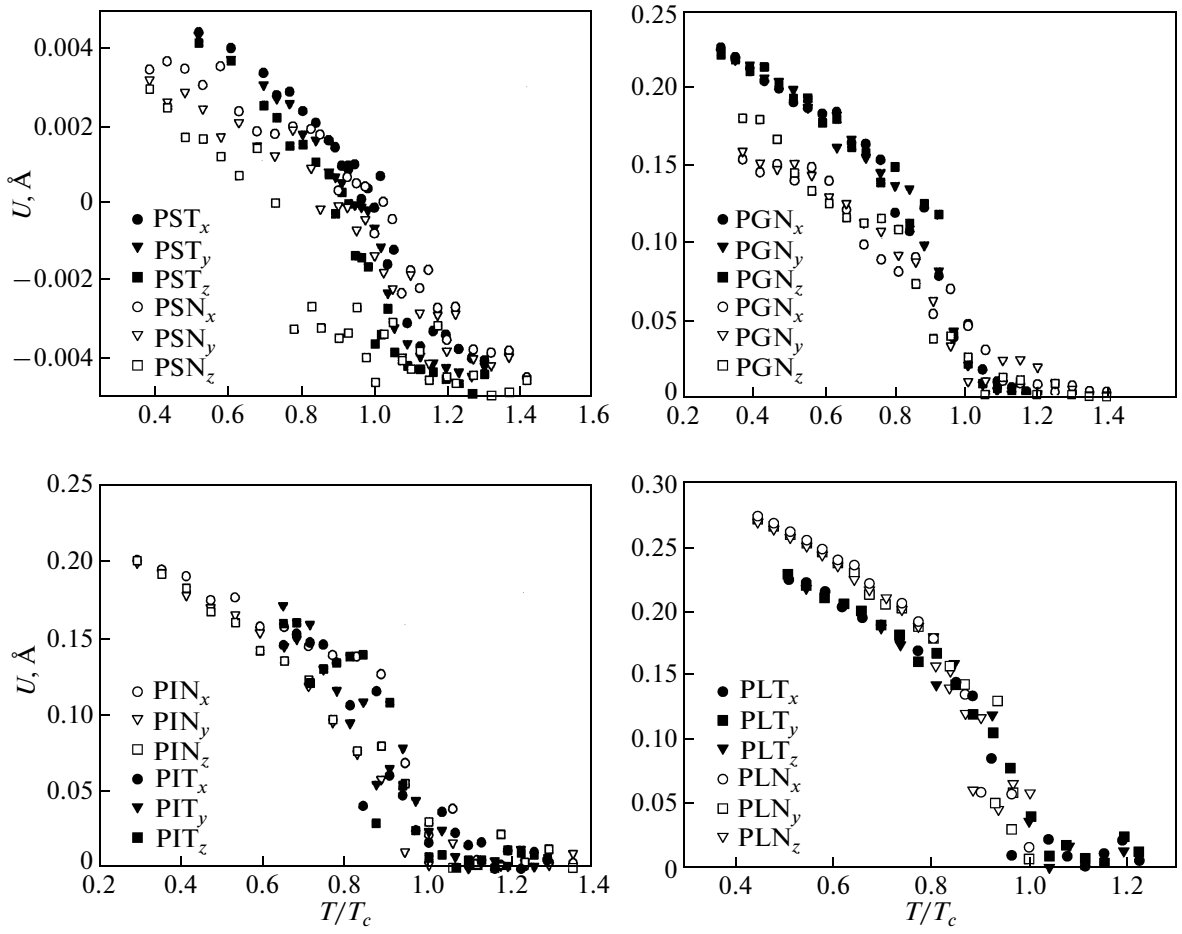

Fig. 3. Temperature dependences of the local mode amplitude for the ordered $Pb_2B'B''O_6$ solid solutions.

shifted to larger amplitudes of the ion displacements from the equilibrium position in the cubic phase; the depth for the niobium compounds is larger than that for the tantalum compounds (the inverse situation is in the disordered compounds [12]).

The ferroelectric phase transition temperatures were calculated by the method of a model Hamiltonian in the local-mode approximation [11, 17, 18],

Table 4. Eigenvectors of the soft ferroelectric mode Γ_{15}

Compound	Pb	B'	B''	$O_\perp$	$O_\parallel$
PSN	0.48	0.4	0.09	–0.31	–0.01
PST	0.54	0.14	0.04	–0.26	–0.21
PGN	0.55	0.17	0.04	–0.3	–0.06
PGT	0.55	0.09	0.04	–0.31	–0.003
PIN	0.56	0.11	0.02	–0.3	–0.02
PIT	0.56	0.08	0.02	–0.3	–0.001
PLN	0.57	0.09	0.01	–0.29	–0.01
PLT	0.55	0.08	0.02	–0.31	–0.015

where the three-component local mode $S^\alpha = u^\alpha \sum_i \xi_{i\alpha}$ (u is the amplitude of ionic displacements, and $\xi_{k\alpha}$ is the eigenvector of the mode from Table 4) was centered on the Pb ions undergoing the largest displacement and placed in the sites of the face-centered cubic lattice. The model Hamiltonian included the energies of the short-range interactions within the limits of the two coordination shells (E_{short}) and long-range dipole–dipole interactions of the local modes (E_{dip}), and also the energy of the single-site anharmonicity (E_{anharm}):

$$E_{\text{tot}} = E_{\text{anharm}}(\{S_i\}) + E_{\text{short}}(\{S_i\}, \{S_j\}) + E_{\text{dip}}(\{S_i\}, \{S_j\}). \quad (1)$$

The explicit expressions for the model Hamiltonian are presented in [11, 17]. The distorted structures used in calculations of the parameters of the effective Hamiltonian for the ordered solid solutions and the procedure of determination of the parameters of the Hamiltonian from the set of energies of the distorted structures are presented in [11]. The calculated

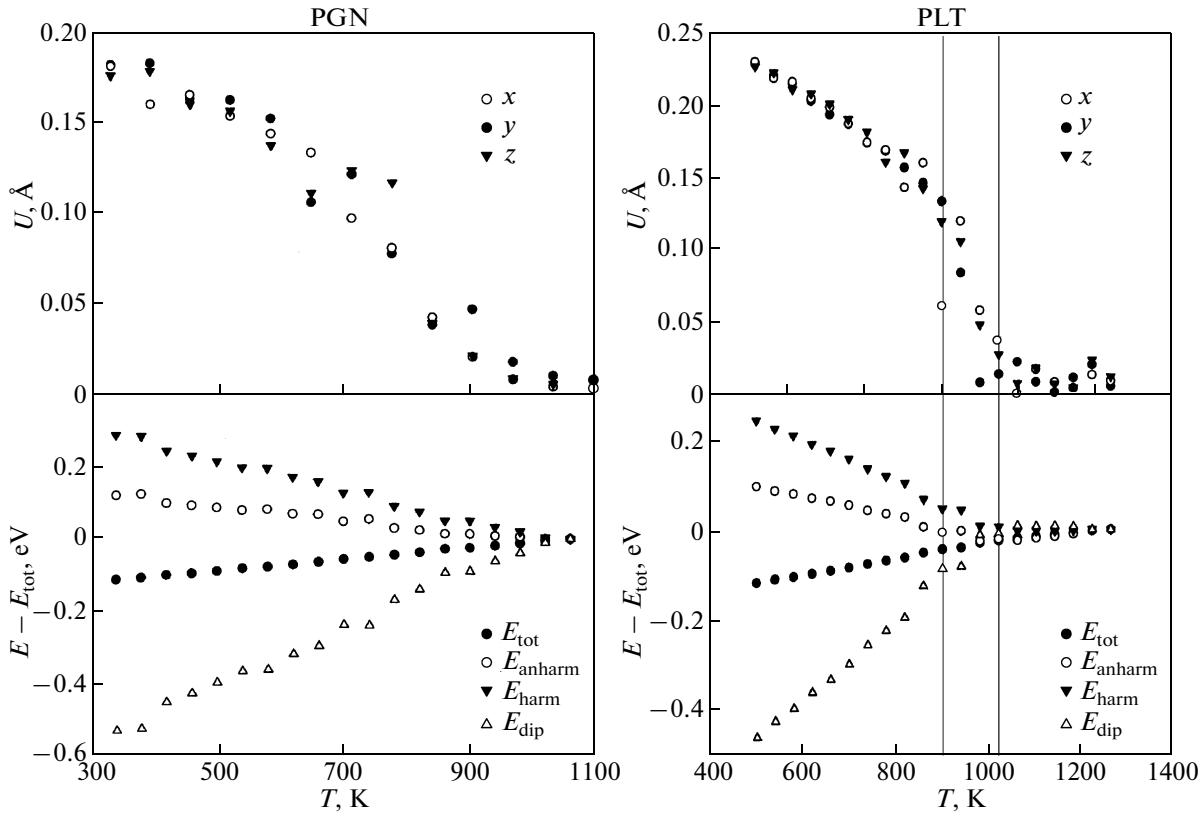

Fig. 4. Temperature dependences of the local mode amplitude and energies for PGN and PLT. At the upper parts of the figure, different symbols correspond to x, y, and z components of the local mode; at the lower parts of the figure, different symbols corresponds to the total energy and different contributions to it.

parameters of the model Hamiltonian for all solid solutions are listed in Table 5.

The temperature behavior of the system with the model Hamiltonian (1) was calculated by the Monte Carlo method using the parameters from Table 5. The Monte Carlo procedure is described in [11], where the ferroelectric transition was calculated in the PSN and PST compounds. The results of the Monte Carlo calculations for all the compounds under discussion are presented in Figs. 3–5 and in Table 5. Figure 3 shows the temperature dependence of three components of the transition parameter. According to the Monte Carlo calculation, the ordered solid solutions undergo the phase transition to the rhombohedral ferroelectric phase with the almost equal nonzero values of the three components of the local mode. In this case, in some solid solutions (e.g., PSN [11] and PLT), the Monte Carlo procedure demonstrates a narrow temperature intermediate region of existence of the ferroelectric phase with two nonzero and equal components of the local mode. It should be noted that it is fairly difficult to determine the transition temperature (T_c) from the temperature dependences of the order parameter according to the Monte Carlo data; and because of this the phase transition temperatures were determined from the temperature dependences of individual contributions to the total internal energy of the system (short-range and dipole–dipole energies), which have marked kinks near the phase transition. The temperature dependences of the energy and individual contributions to it calculated by the Monte Carlo method for PSN and PST are presented in [11]. Similar dependences are observed also for other compounds of the solid solution under consideration, because of this we show in Fig. 4 as examples and in order to save room the results only for PGN and PLT, where, in the former case, there is only one transition from the paraelectric to the ferroelectric phase, and, in the latter case, as mentioned above, there is a narrow temperature range with two nonzero components of the order parameter. Table 5 lists the temperatures of the phase transitions from the cubic phase to the rhombohedral phase and values of the spontaneous polarization in this phase obtained by the Monte Carlo method. Figure 5 depicts the temperature dependences of the spontaneous polarization in the ferroelectric phase. As seen from the figure, the kinks in the temperature dependences of the spontaneous polarization approximately agree with the transition temperatures determined from the temperature dependences of the energy (Table 5). Despite the fairly small

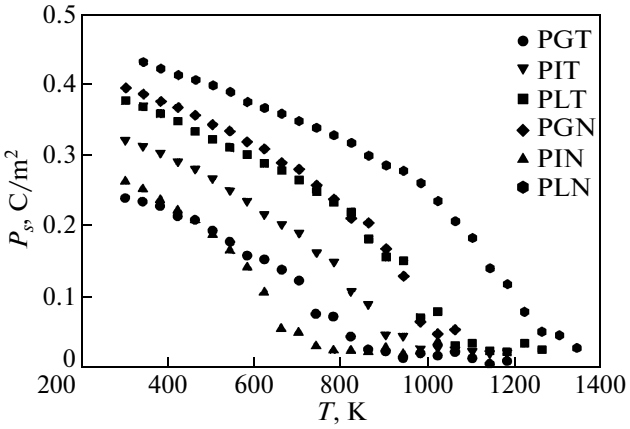

Fig. 5. Temperature dependences of the spontaneous polarization of the $Pb_2B'B''O_6$ solid solutions.

scatter in the parameters of the model Hamiltonian for different compositions, as seen from Table 5, the scatter of the transition temperatures is about 1000 K, namely, from 490 to 1380 K. It should be noted that the obtained temperatures are higher than the temperatures of the ferroelectric phase transition for the disordered solid solutions calculated in [12]. It is seen from Table 5 that the ferroelectric transition temperature increases with increasing atomic number of the B' ion in both niobium and tantalum compounds (exception for PGN which drops out of the series). In this case, the ferroelectric phase of tantalum $PbB'_{1/2}Ta_{1/2}O_3$ solid solutions is stabilized at higher temperatures than that in $PbB'_{1/2}Nb_{1/2}O_3$, with the exception of the PGN and PGT pairs and PLN and PLT pairs, for which situation is inverse. Similar behavior is observed also for the spontaneous polarization. A possible reason for the increase in the transition temperature with an increase in the atomic mass of the B' ion was indicated in [12], where this behavior was attributed to the increase in the energy of the dipole–dipole interactions, which, in turn, was assumed to be related to large displacement amplitudes for the compounds with the large atomic number of the B' ion.

In conclusion, the results obtained in this work can be briefly summarized as follows.

(1) The calculated lattice vibration spectrum of the ordered $Pb_2B'B''O_6$ (B' = Ga, In, Lu; B'' = Nb, Ta) solid solutions with the elpasolite structure contains the unstable modes responsible for the instability of the lattice with respect to the polar vibrations (Γ_{15} mode). In all the compounds, these modes are close in frequency. In the eigenvectors of these modes, the lead ions are mainly displaced.

(2) In the local mode approximation, we determined the parameters of the effective Hamiltonian which describes the ferroelectric phase transition and calculated the transition temperature for all the solid solutions under consideration. It was found that, in the compounds containing B' ions with a large atomic number, the transition temperature increases. A similar dependence was obtained for the calculated value of the spontaneous polarization.

Table 5. Parameters of the model Hamiltonian (eV) (a_1–a_3, b_1, and b_2 are the parameters of the short-range interaction; A, B, and C are the parameters of the single-site anharmonicity); Z is the effective charge of the mode (in units of e), ferroelectric phase transition temperatures T_c, and spontaneous polarizations P_s

Parameter	PSN	PGN	PIN	PLN	PST	PGT	PIT	PLT
a_1	−44.68	−40.16	−34.23	−29.69	−44.68	−34.71	−35.92	−34.00
a_2	87.24	74.63	61.09	52.35	87.24	58.76	61.72	59.42
a_3	152.17	128.56	102.99	83.70	152.17	111.53	100.73	92.67
b_1	14.76	9.98	3.91	−1.56	14.76	3.40	6.08	2.98
b_2	−14.52	−5.82	−4.26	−3.71	−14.52	−5.06	−5.21	−5.22
A	180	146.89	121.21	105.76	180	118.32	112.41	104.36
B	5880	8158	9155	9381	5880	9484	8992	9979
C	8411	7751	9337	8290	8411	10652	9949	7464
Z	5.28	5.20	4.40	4.22	7.41	4.33	4.21	4.25
Ferroelectric phase transition temperature T_c, K								
Calculation	490	980	760	1480	610	820	930	1060
Experiment	350 [19]	–		–	300 [19]	–		–
Spontaneous polarization P_s, C/m^2								
Calculation	0.24	0.41	0.28	0.44	0.24	0.25	0.33	0.38
Experiment	–	–	–	–	0.26 [19]	–	–	–

ACKNOWLEDGMENTS

This study is supported by the Russian Foundation for Basic Research (project no. 09-02-00067) and the Council on Grants from the President of the Russian Federation for Support of the Leading Scientific Schools (grant no. NSh-4137.2006.2).

REFERENCES

1. Y. Park, K. M. Knowles, and K. Cho, Phase Transform. **68**, 411 (1999).
2. K. Nomura, T. Shingai, N. Yasuda, H. Ohwa, and H. Terauchi, Ferroelectrics **218**, 69 (1998).
3. A. A. Bokov, I. P. Rayevsky, V. V. Neprin, and V. G. Smotrakov, Ferroelectrics **124**, 271 (1991).
4. V. A. Shuvaeva, Y. Azuma, I. P. Raevski, K. Yagi, K. Sakaue, and H. Terauchi, Ferroelectrics **299**, 103 (2004).
5. P. Groves, Phase Transform. **6**, 115 (1986).
6. P. Groves, J. Phys. C: Solid State Phys. **19**, 5103 (1986).
7. A. Kania, K. Roleder, G. E. Kugel, and M. Hafid, Ferroelectrics **135**, 72 (1992).
8. V. A. Isupov, Ferroelectrics **289**, 131 (2003).
9. *Ferroelectrics and Antiferroelectrics*, Ed. by G. A. Smolenskiĭ (Nauka Moscow, 1971) [in Russian].
10. V. I. Zinenko, N. G. Zamkova, E. G. Maksimov, and S. N. Sofronova, Zh. Éksp. Teor. Fiz. **132** (3), 702 (2007) [JETP **105** (3), 617 (2007)].
11. V. I. Zinenko and N. G. Zamkova, Zh. Éksp. Teor. Fiz. **133** (3), 622 (2008) [JETP **106** (3), 542 (2008)].
12. V. S. Zhandun, N. G. Zamkova, and V. I. Zinenko, Zh. Éksp. Teor. Fiz. **133** (6), 1266 (2008) [JETP **106** (6), 1109 (2008)].
13. E. G. Maksimov, V. I. Zinenko, and N. G. Zamkova, Usp. Fiz. Nauk **174** (11), 1145 (2004) [Phys.—Usp. **47** (11), 1075 (2004)].
14. C. Perrin, N. Menguy, O. Bidault, C. Y. Zahra, A.-M. Zahra, C. Caranoni, B. Hilczer, and A. Stepanov, J. Phys.: Condens. Matter **13**, 10231 (2001).
15. C. G. F. Stenger and A. J. Burggraaf, Phys. Status Solidi A **61**, 275 (1980).
16. A. Kania and N. Pavlaczyk, Ferroelectrics **124**, 261 (1991).
17. U. V. Waghmare and K. M. Rabe, Phys. Rev. B: Condens. Matter **55**, 6161 (1997).
18. W. Zhong and D. Vanderbilt, Phys. Rev. B: Condens. Matter **52**, 6301 (1995).
19. C. Malibert, B. Dkhil, J. M. Kiat, D. Durand, J. F. Bérar, and A. Spasojevic-de Biré, J. Phys.: Condens. Matter **9**, 7485 (1997).

Translated by Yu. Ryzhkov